Joint ITS- and IRS-Assisted Cell-Free Networks

Zheng Chu, *Member, IEEE*, Pei Xiao, *Senior Member, IEEE*, Chuan Heng Foh, *Senior Member, IEEE* De Mi, *Senior Member, IEEE*, Kanapathippillai Cumanan, *Senior Member, IEEE*, and Alister Graham Burr, *Senior Member, IEEE*

***Abstract*—This paper investigates a joint intelligent transmissive surface (ITS) and intelligent reflecting surface (IRS)-assisted cell-free network. Specifically, various ITS-assisted base stations (BSs), handled via a central processing unit (CPU), broadcast information signals to multiple IoT devices, carried by active transmit beamforming and transmissive reflecting phase shifts. Meanwhile, an IRS passively reflect signals from the ITS-assisted BS to the IoT devices. To examine this network performance, a sum rate is maximized among all users to jointly optimize the active beamforming, ITS and IRS passive beampatterns. These coupled variables leads to the non-convexity of this formulated optimization problem, which cannot be directly solved. To deal with this issue, we begin with applying the Lagrange dual transformation (LDT) and quadratic transformation (QT) to recast the sum of multiple logarithmically fractional objectives to the subtractive form, and further to quadratic form. Next, an alternating optimization (AO) algorithm is presented to separately the active beamforming, ITS and IRS passive beampatterns in an iterative fashion. Each sub-optimal solution of these variables can be iteratively derived, in a closed-form, by solving the quadratic objective function with a convex constraint or a unit-modulus constraint via the dual method with bisection search or the Alternating Direction Method of Multipliers (ADMM) algorithm. Finally, simulation results are provided to confirm the performance of the proposed algorithm compared to several benchmark schemes.**

***Index Terms*—Cell-free networks, intelligent reflecting/transmissive surface (IRS/ITS), Lagrange dual transformation (LDT), quadratic transformation (QT), and alternating direction method of multipliers (ADMM).**

I. Introduction

Wireless communication technologies have undergone remarkable evolution over the past decades, leading to transformative advancements. With the successful rollout of the fifth-generation (5G) technology, attention is already shifting towards the sixth-generation (6G) networks, anticipated as the next leap in wireless communications. The vision for 6G is to achieve even higher data rates, reduced latency, and support more diverse use cases [1]. It aims to establish an ultra-reliable and ubiquitous connectivity fabric that interconnects not only humans but also devices, machines, and intelligent systems, ushering in the Internet of Everything (IoE) era [2].

This work was supported in part by the U.K. Engineering and Physical Sciences Research Council under Grant EP/X013162/1 and EP/X01309X/1.

Z. Chu was with the Institute for Communication Systems (ICS), Home for 5GIC & 6GIC, University of Surrey, Guildford, Surrey, GU2 7XH, United Kingdom, and is now with the Department of Electrical and Electronic Engineering, University of Nottingham Ningbo China, Ningbo 315100, China. (Email: andrew.chuzheng7@gmail.com)

P. Xiao, and C. Foh are with the Institute for Communication Systems (ICS), Home for 5GIC & 6GIC, University of Surrey, Guildford, Surrey, GU2 7XH, United Kingdom. (Email: p.xiao@surrey.ac.uk; c.foh@surrey.ac.uk)

D. Mi is with the School of Computing and Digital Technology, Birmingham City University, Birmingham B4 7XG, United Kingdom. (Email: de.mi@bcu.ac.uk)

K. Cumanan and Alister G. Burr are with the School of Physics, Engineering and Technology, University of York, York YO10 5DD, United Kingdom. (Email: kanapathippillai.cumanan@york.ac.uk; alister.burr@york.ac.uk).

Cell-free massive multiple-input multiple-output (MIMO), as one of the potential paradigms for 6G networks, is composed of multiple distributed base stations (BSs), which serve a number of users/devices, such that great performance for all devices can be guaranteed, especially cell-edge ones [3]. To improve network capacity and meet the challenge of BS deployment cost, the intelligent reflecting surface (IRS) and intelligent transmissive surface (ITS) are considered to build favorable channel propagation [4], both consist of a large number of low-cost passive elements/arrays aiming to control their individual amplitude and phase shift to dynamically varying these units such that the incident signal could be reshaped in the reflective and refractive manners, respectively.

Recently, existing research endeavors have been contributed to the IRS/ITS-empowered wireless networks to design the maximum weighted sum rate (WSR) by optimizing the active transmit beamforming, IRS and ITS passive beampatterns [4]. Also, joint ITS- and IRS-aided secure communication was studied in [5] to alternately design active beamforming of BS and passive beampattern of IRS/ITS so as to maximize the sum secrecy capacity. Several research works studied the IRS-assisted cell-free MIMO systems that can further improve the performance of cell-free MIMO systems at low cost and energy consumption [6], [7]. In [8], a cooperative beamforming was introduced in the IRS-assisted cell-free MIMO system. The fully decentralized design framework was presented for cooperative beamforming [6], while the hybrid beamforming (HBF) scheme was considered to design BS-based digital beamforming as well as IRS-based passive beamforming [7]. Very recently, the IRS has been considered in a cell-free massive MIMO context with hardware impairments (HWIs) and imperfect channel state information (CSI) [9], where a tight closed-form expression was derived based on these practical assumptions and the trade-off performance was analyzed to reflect on the impact of BSs' and IRSs' numbers.

Although the existing research focuses on the application of IRS/ITS in different wireless contexts, the potentials of joint IRS and ITS have not been fully investigated. Specifically, multiple distributed BSs are typically equipped with a large number of active radio frequency (RF) chains, which brings a very high power consumption and hardware cost, with the increasing number of antennas. In cellular networks, cell edge users do not have a sufficiently strong signal reception due to the severe pathloss and aggregated interference [10]. Hence, more research efforts are needed to address problems, such as, how we design a novel system aiming to effectively reduce hardware cost and energy consumption, and at the same time, improve network coverage and signal reception in the cell-free network. These full potentials can be unlocked by exploiting an integration of ITS and IRS, which not only reduces hardware design cost and improves energy efficiency (EE), but also enhances information transmission and network coverage capabilities, by creating favorable wireless propagations and

in cell-free networks with a sporadic distribution of BSs.

We propose a joint application of IRS and ITS in a cell-free context, where several distributed ITS-assisted BSs are coordinately deployed to serve multiple IoT devices with the help of an IRS. *The main contributions of this paper are summarized as follows:*

- First, we characterize the ITS-assisted cell-free architecture, which conceives a novel ITS-assisted transceiver to reduce the hardware design cost induced by the analogue active beamforming at the BS, and to improve the network energy efficiency (EE). Also, the IRS is deployed to act as a passive relay in the wireless network to create a cascaded link from ITS to IoT devices via IRS, which enhances the quality of signal reception and network coverage. In this work, we fully unlock the potentials of IRS and ITS to design the integrated ITS-assisted transceiver structure and IRS in the cell-free network. To the best of our knowledge, this work is the first of its kind to investigate the joint ITS- and IRS-assisted cell-free context. To examine the system performance, the sum rate is maximized aiming to design the active beamforming of BS, and IRS/ITS passive beampatterns.[1]
- Since the formulated problem involves multiple coupled variables such that it is not jointly convex and cannot be solved directly. In what follows, we focus on developing a suitable optimization strategy, i.e., alternating optimization (AO) algorithm, to iteratively solve this problem. First, we utilize the Lagrange dual transformation (LDT) and the quadratic transformation (QT) to equivalently convert the sum of multiple logarithmically objective functions into quadratic programming. For given IRS and ITS beampatterns, we exploit the dual method to derive the semi-closed-form solution of active beamforming with a bisection search over the dual variable. Then, for the given active beamforming, we present an ADMM algorithm to iteratively design the semi-closed-form solution of IRS/ITS phase shifts.[2] Moreover, the computational complexity of the proposed algorithm is characterized.

II. System Model

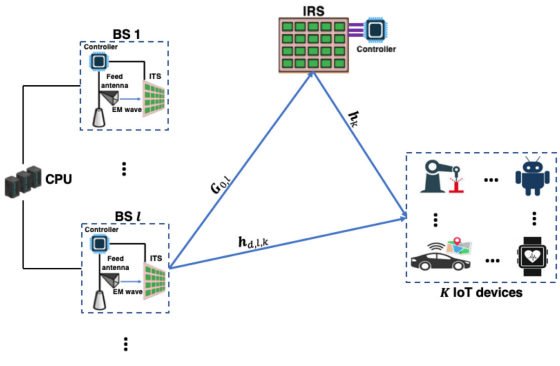

Fig. 1: System model.

This paper first introduces a cell-free network assisted by multiple ITSs and an IRS. Specifically, it consists of L ITS-assisted BSs, where the l-th BS and ITS are equipped with $N_{B,l}$ and $N_{T,l}$, $\forall l \in [1, L]$ active antennas and passive transmissive elements, respectively, satisfying $\sum_{l=1}^{L} N_{B,l} = N_B$ and $\sum_{l=1}^{L} N_{T,l} = N_T$, an IRS is equipped with N_R reflecting elements as well as K single-antenna IoT devices.

The l-th ITS-assisted BSs broadcast the active beamforming, i.e., $\mathbf{w}_{l,k} \in \mathbb{C}^{N_{B,l}\times 1}$ coupled with signal transmission coefficient, i.e., $\mathbf{\Theta}_{T,l} = \text{diag}\left[\theta_{T,l,1}, ..., \theta_{T,l,n_{T,l}}, ..., \theta_{T,l,N_{T,l}}\right]$, $\forall n_{T,l} \in [1, N_{T,l}]$ to the k-th IoT device under the help of the IRS with its reflection coefficient, i.e., $\mathbf{\Theta}_R = \text{diag}\left[\theta_{R,1}, ..., \theta_{R,n_R}, ..., \theta_{R,N_R}\right]$. All of ITS-assisted BSs are coordinated by a central processing unit (CPU). The transmission and reflection coefficients are denoted by $\theta_{T,l,n_{T,l}/R,n_R} = \beta_{T,l,n_{T,l}/R,n_R} \exp(j\alpha_{T,l,n_{T,l}/R,n_R})$, $\beta_{T,l,n_{T,l}/R,n_R} = 1$ and $\alpha_{T,l,n_{T,l}/R,n_R} \in [0, 2\pi)$, where $\beta_{T,l,n_{T,l}/R,n_R}$ and $\alpha_{T,l,n_{T,l}/R,n_R}$ are the phase shifts and amplitudes of ITSs and IRS, respectively. All ITSs and IRS perform passive transmission and reflection by dynamically adjusting their own phase shift, as well as maximizing transmissive and reflecting signal gains, respectively.[3] To characterize the maximum network performance and without loss of generality, it is assumed that all CSI can be effectively estimated and obtained by the ITS-assisted BSs. We denote the channel coefficients between BS l and ITS l, ITS l and IRS, IRS and IoT device k, as well as ITS l and IoT device k as $\mathbf{S}_l \in \mathbb{C}^{N_{T,l}\times N_{B,l}}$, $\mathbf{G}_{0,l} \in \mathbb{C}^{N_R\times N_{T,l}}$, $\mathbf{h}_k \in \mathbb{C}^{N_R\times 1}$, and $\mathbf{h}_{d,k,l} \in \mathbb{C}^{N_{T,l}\times 1}$, respectively.[4] We consider that the transmit antenna and transmissive elements of each BS and ITS are arranged in uniform linear array (ULA) [19]. The channel of the l-th BS-ITS link $\mathbf{S}_l$ is considered as a near-field channel [20], where a three-dimensional (3-D) topology is considered to characterize the channel coefficient. The central point of BS l antenna can be denoted as $(0, 0, l_{BS} \times a)$ if $l_{BS} = 1, ..., (2 * l + 1)$ or $(0, 0, -(l_{BS} - 1) \times a)$ if $l_{BS} = 2, ..., 2 * l$, where a is the interval between two adjacent BSs. It is assumed that the coordinate of m_l-th antenna of BS can be denoted as $(0, \tilde{m}_{ITS,l} * d_{ap}, l_{BS} \times a)$ or $(0, \tilde{m}_{ITS,l} * d_{ap}, -(l_{BS} - 1) \times a)$, where $\tilde{m}_{ITS,l} = m_l - \frac{N_{B,l}-1}{2}$ and d_{ap} represents the antenna pitch. We denote the coordinate of the $n_{T,l}$-th antenna of ITS l as $(x_{ITS,l}, y_{ITS,l} + \tilde{m}_{ITS,l} d_{ap}, l_{ITS} \times a)$ if $l_{ITS} = 1, ..., (2 * l + 1)$ or $(x_{ITS,l}, y_{ITS,l} + \tilde{m}_{ITS,l} d_{ap}, -(l_{ITS} - 1) \times a)$ if $l_{ITS} = 2, ..., 2 * l$.The near-field distance between the m_l-th antenna of BS l and the $n_{T,l}$-element of ITS l can be derived as $d_{m_l,n_{T,l}} = \sqrt{x_{ITS,l}^2 + [\tilde{m}_{ITS,l} d_{ap} - (y_{ITS,l} + \tilde{m}_{ITS,l} d_{ap})]^2}$. Thus, the line-of-sight (LoS) near-field channel coefficient between the BS l and ITS l can be modeled as

[1]Sum rate maximization was considered in [11], however, in a different context from this work, i.e., IRS-assisted MISO downlink system, where designed BS active and IRS passive beamforming alternately.

[2]Unlike [11], our work investigates the ADMM algorithm to iteratively optimize the IRS/ITS phase shifts, rather than using the Compute Riemannian Gradient (CRG).

[3]In our work, the IRS plays a passively reflective role in improving the received power at the users by creating a cascaded channel of BS-IRS-user link to assist the weak direct link; the ITS acts as a passive transmitter to support BS for information transmission. The ITS-assisted counterpart relies on a near-field cascaded link to improve EE performance and reduce the transceiver design cost due to its passive nature.

[4]The channel estimation techniques, i.e., message passing (MP) algorithm, channel correlation method, optimization-based channel estimation algorithm, decomposition, interpolation recovery, etc., can be utilized for the cascaded link [12]–[15]. In addition, to evaluate the impact of channel uncertainty on the sum rate performance, the imperfect CSI can be considered as the bounded or statistical model introduced in [16]–[18], where it shows that the CSI uncertainty or channel estimation error model can degrade achievable rate performance.

$\mathbf{S}_l = \left[\mathbf{s}_{l,1}, ..., \mathbf{s}_{l,N_{T,l}}\right]^T$, where $\mathbf{s}_{l,n_{T,l}}$ can be written as (1) at the top of next page. [5] For the l-th ITS-assisted BS, its transmitted signal can be denoted by $\mathbf{x}_l = \mathbf{\Theta}_{T,l}\mathbf{S}_l \sum_{j=1}^{K} \mathbf{w}_{l,j} s_j$, where $s_j \in \mathbb{C}^{1\times 1}$ is the transmitted symbol for the k-th IoT device satisfying $\mathbb{E}\left\{|s_j|^2\right\} = 1$. Thus, the received signal at the k-th IoT device can be given by $y_k = \left(\mathbf{h}_{d,k}^H + \boldsymbol{\theta}_R^H \mathbf{G}_k\right) \mathbf{\Theta}_T \mathbf{S} \mathbf{w}_k s_k + \left(\mathbf{h}_{d,k}^H + \boldsymbol{\theta}_R^H \mathbf{G}_k\right) \mathbf{\Theta}_T \mathbf{S} \sum_{j\neq k} \mathbf{w}_j s_j + n_k$,where $n_k \sim \mathcal{CN}\left(0, \sigma_k^2\right)$ denotes the additive Gaussian white noise at the k-th IoT device; $\mathbf{G}_k = \text{diag}\left(\mathbf{h}_k^H\right)\mathbf{G}_0$, $\mathbf{h}_{d,k}^H = \left[\mathbf{h}_{d,1,k}^H, ..., \mathbf{h}_{d,L,k}^H\right]$, $\mathbf{G}_0 = [\mathbf{G}_{0,1}, ..., \mathbf{G}_{0,L}]$, $\mathbf{S} = \left[\tilde{\mathbf{S}}_1, ..., \tilde{\mathbf{S}}_L\right]$, $\boldsymbol{\theta}_R^H = [\theta_{R,1}, ..., \theta_{R,N_R}]$, $\mathbf{w}_j = \left[\mathbf{w}_{1,k}^H \ \cdots \ \mathbf{w}_{L,j}^H\right]^H$, $\mathbf{w} = \left[\mathbf{w}_1^H \ \cdots \ \mathbf{w}_K^H\right]^H$, $\mathbf{\Theta}_T = \text{diag}\left[\mathbf{\Theta}_{T,1}, ..., \mathbf{\Theta}_{T,L}\right]$, and $\tilde{\mathbf{S}}_l = \left[\mathbf{o}_{N_{T,1}\times N_{B,l}}^H, \cdots, \mathbf{o}_{N_{T,l-1}\times N_{B,l}}^H, \mathbf{s}_l^H, \mathbf{o}_{N_{T,l+1}\times N_{B,l}}^H, \cdots, \mathbf{o}_{N_{T,L}\times N_{B,l}}^H\right]^H$. Accordingly, the achievable rate of the k-th IoT device is expressed as $R_k = \log\left(1 + \frac{\left|\left(\mathbf{h}_{d,k}^H + \boldsymbol{\theta}_R^H \mathbf{G}_k\right)\mathbf{\Theta}_T \mathbf{S}\mathbf{w}_k\right|^2}{\sum_{j\neq k}\left|\left(\mathbf{h}_{d,k}^H + \boldsymbol{\theta}_R^H \mathbf{G}_k\right)\mathbf{\Theta}_T \mathbf{S}\mathbf{w}_j\right|^2 + \sigma_k^2}\right)$. In this work, we aim to formulate the sum rate maximization problem as follows:

$$\max_{\mathbf{w}, \mathbf{\Theta}_T, \boldsymbol{\theta}_R} \ f_1\left(\mathbf{w}, \mathbf{\Theta}_T, \boldsymbol{\theta}_R\right) = \sum_{k=1}^{K} R_k \tag{2a}$$

$$s.t. \ \sum_{k=1}^{K} \|\mathbf{w}_k\|^2 \leq P, \tag{2b}$$

$$\left|\theta_{T/R, n_T/n_R}\right| = 1, \forall n_T/n_R. \tag{2c}$$

Problem (2) consists of multiple coupled variables in terms of active and passive beamforming $\mathbf{w}$, and $\mathbf{\Theta}_T$ as well as $\boldsymbol{\theta}_R$, respectively, which leads to its non-convexity and cannot be solved directly. To circumvent this issue, we propose an AO algorithm to iteratively solve this problem in the following.

III. Solution to Problem (2)

This section aims to solve problem (2) in an alternating fashion. We first consider the LDT to transform the sum of multiple logarithmic objective functions in (2a) into a sum of multiple fractional counterparts. To proceed, let us introduce $\boldsymbol{\nu} = [\nu_1, ..., \nu_K]$ as an auxiliary variables, and the objective function (2a) is recast as $f_1\left(\mathbf{w}, \mathbf{\Theta}_T, \boldsymbol{\theta}_R\right) = \sum_{k=1}^{K} \log\left(1+\nu_k\right) - \nu_k + \frac{(1+\nu_k)\eta_k}{1+\eta_k}$, where $\eta_k = \frac{\left|\left(\mathbf{h}_{d,k}^H + \boldsymbol{\theta}_R^H \mathbf{G}_k\right)\mathbf{\Theta}_T \mathbf{S}\mathbf{w}_k\right|^2}{\sum_{j\neq k}\left|\left(\mathbf{h}_{d,k}^H + \boldsymbol{\theta}_R^H \mathbf{G}_k\right)\mathbf{\Theta}_T \mathbf{S}\mathbf{w}_j\right|^2 + \sigma_k^2}$. We alternately optimize the variables $\boldsymbol{\nu}$ and $\left(\mathbf{w}, \mathbf{\Theta}_T, \boldsymbol{\theta}_R\right)$. For given $\left(\mathbf{w}, \mathbf{\Theta}_T, \boldsymbol{\theta}_R\right)$, we take the first-order derivative $\frac{\partial f_1}{\partial \nu_k} = 0$ to obtain the close-form solution of ν_k as

$$\nu_k^* = \eta_k. \tag{3}$$

For given $\boldsymbol{\nu}$, the variables $\left(\mathbf{w}, \mathbf{\Theta}_T, \boldsymbol{\theta}_R\right)$ can be optimized by solving problem (4)

$$\max_{\mathbf{w}, \mathbf{\Theta}_T, \boldsymbol{\theta}_R} \ \sum_{k=1}^{K} \frac{(1+\nu_k)\left|\left(\mathbf{h}_{d,k}^H + \boldsymbol{\theta}_R^H \mathbf{G}_k\right)\mathbf{\Theta}_T \mathbf{S}\mathbf{w}_k\right|^2}{\sum_{i=1}^{K}\left|\left(\mathbf{h}_{d,k}^H + \boldsymbol{\theta}_R^H \mathbf{G}_k\right)\mathbf{\Theta}_T \mathbf{S}\mathbf{w}_i\right|^2 + \sigma_k^2}, \tag{4a}$$

$$s.t. \ (2b), \ (2c). \tag{4b}$$

Note that (4) is still intractable due to the fractionality of its objective function (4a). Thus, we apply an AO algorithm to alternately design $\mathbf{w}_k$, $\mathbf{\Theta}_R$, and $\boldsymbol{\theta}_T$. To proceed, we present the QT to recast the fractional objective function (4a) into the subtractive form. Let $\mathbf{h}_k^H = \left(\mathbf{h}_{d,k}^H + \boldsymbol{\theta}_R^H \mathbf{G}_k\right)\mathbf{\Theta}_T \mathbf{S}$, and we introduce an auxiliary variable $\boldsymbol{\omega} = [\omega_1, ...\omega_K]$,

$$\max_{\boldsymbol{\omega}, \mathbf{w}, \boldsymbol{\theta}_R, \mathbf{\Theta}_T} \ \sum_{k=1}^{K} 2\sqrt{(1+\nu_k)}\Re\left\{\text{conj}\left(\omega_k\right)\mathbf{h}_k^H \mathbf{w}_k\right\} - \sum_{k=1}^{K}|\omega_k|^2\left(\sum_{j=1}^{K}\left|\mathbf{h}_k^H \mathbf{w}_i\right|^2 + \sigma_k^2\right),$$
$$s.t. \ (2b), \ (2c). \tag{5}$$

For given $\mathbf{w}_k$, $\boldsymbol{\theta}_R$, and $\mathbf{\Theta}_T$, $\boldsymbol{\omega}$ can be derived in closed-form, as

$$\omega_k^* = \frac{\sqrt{1+\nu_k}\left(\mathbf{h}_k^H \mathbf{w}_k\right)}{\sum_{i=1}^{K}\left|\mathbf{h}_k^H \mathbf{w}_i\right|^2 + \sigma_k^2}. \tag{6}$$

For given $\boldsymbol{\omega}$, in the sequel, we continue to solve problem (5) with respect to $\mathbf{w}_k$, $\boldsymbol{\theta}_R$, and $\mathbf{\Theta}_T$ in an alternating manner.

A. Solution of Active Beamforming

Now, let us solve problem (5) in terms of the active beamforming $\mathbf{w}_k$ for given $\boldsymbol{\theta}_R$ and $\mathbf{\Theta}_T$. To proceed, we first consider the Lagrange dual function of (5) in terms of $\mathbf{w}_k$ as $\mathcal{L}\left(\mathbf{w}, \lambda\right) = \sum_{k=1}^{K} 2\sqrt{(1+\nu_k)}\Re\left\{\text{conj}\left(\omega_k\right)\mathbf{h}_k^H \mathbf{w}_k\right\} - \sum_{k=1}^{K}|\omega_k|^2\left(\sum_{j=1}^{K}\left|\mathbf{h}_k^H \mathbf{w}_i\right|^2 + \sigma_k^2\right) - \lambda\left(\sum_{k=1}^{K}\|\mathbf{w}_k\|^2 - P\right)$, where $\lambda \geq 0$ is the dual variable of constraint (2b). By manipulating $\frac{\partial \mathcal{L}}{\partial \mathbf{w}_k} = 0$, we have

$$\mathbf{w}_k^* = \sqrt{1+\nu_k}\omega_k\left(\lambda \mathbf{I} + \sum_{k=1}^{K}|\omega_k|^2 \mathbf{h}_k \mathbf{h}_k^H\right)\mathbf{h}_k, \tag{7}$$

where λ can be obtained by the bisection method to solve the following problem:

$$\lambda^* = \left\{\lambda \geq 0 : \sum_{k=1}^{K} \mathbf{w}_k^H \mathbf{w}_k = P\right\}. \tag{8}$$

B. Solution of IRS and ITS Beampatterns

Here, we first fix the active beamforming $\mathbf{w}$ and the ITS beampattern $\mathbf{\Theta}_T$ to optimize the IRS phase shifts $\boldsymbol{\theta}_R$ by solving problem (5). With some mathematical manipulations, we rewrite (5) into a quadratic form with respect to $\boldsymbol{\theta}_R$, as

$$\min_{\boldsymbol{\theta}_R} \boldsymbol{\theta}_R^H \mathbf{B}_R \boldsymbol{\theta}_R - 2\Re\left\{\boldsymbol{\theta}_R \boldsymbol{\gamma}_R\right\}, s.t. \left|\theta_{R,n_R}\right| = 1, \forall n_R, \tag{9}$$

where $a_{k,i} = \mathbf{h}_{d,k}^H \mathbf{\Theta}_T \mathbf{S}\mathbf{w}_i$, $\mathbf{b}_{k,i} = \mathbf{G}_k \mathbf{\Theta}_T \mathbf{S}\mathbf{w}_i$, $\mathbf{B}_R = \sum_{k=1}^{K}|\xi_k|^2 \sum_{i=1}^{K}\mathbf{b}_{k,i}\mathbf{b}_{k,i}^H$, and $\boldsymbol{\gamma}_R = \sum_{k=1}^{K}\left(\sqrt{1+\nu_k}\text{conj}(\xi_k)\mathbf{b}_{k,k} - |\xi_k|^2 \sum_{i=1}^{K}\text{conj}(a_{k,i})\mathbf{b}_{k,i}\right)$. Problem (9) has a quadratic objective with a unit-modulus constraint, resulting in a challenge solution. Thus, we present the ADMM algorithm to iteratively design the IRS beampattern $\boldsymbol{\theta}_R$. This has been investigated in our previous works [4], [21], which is thus omitted here.

Then, we fix the active beamforming $\mathbf{w}$ and the IRS beampattern $\boldsymbol{\theta}_R$ to iteratively design the ITS phase shifts $\mathbf{\Theta}_T$. To proceed, we use $\left|\left(\mathbf{h}_{d,k}^H + \boldsymbol{\theta}_R^H \mathbf{G}_k\right)\mathbf{\Theta}_T \mathbf{S}\mathbf{w}_i\right|^2 = \boldsymbol{\theta}_T^H \mathbf{c}_{k,i}$, where $\mathbf{c}_{k,i} = \text{diag}\left(\left(\mathbf{h}_{d,k}^H + \boldsymbol{\theta}_R^H \mathbf{G}_k\right)^H\right)\mathbf{S}\mathbf{w}_i$. Next, we similarly rewrite (5) into the following problem with respect to $\boldsymbol{\theta}_T$ as

$$\min_{\boldsymbol{\theta}_T} \boldsymbol{\theta}_T^H \mathbf{B}_T \boldsymbol{\theta}_T - 2\Re\left\{\boldsymbol{\theta}_T^H \boldsymbol{\gamma}_T\right\}, s.t. \left|\theta_{T,n_T}\right| = 1, \ \forall n_T, \tag{10}$$

where $\mathbf{B}_T = \sum_{k=1}^{K}|\rho_k|^2 \sum_{i=1}^{K}\mathbf{c}_{k,i}\mathbf{c}_{k,i}^H$, and $\boldsymbol{\gamma}_T = \sum_{k=1}^{K}\sqrt{1+\nu_k}\text{conj}(\rho_k)\mathbf{c}_{k,k}$. Similar to problem (9), (10) also consists a quadratic objective function with a unit-modulus constraint, which is iteratively solved by the ADMM algorithm to obtain the optimal solution of ITS phase shift vector $\boldsymbol{\theta}_T$.

[5] $\left|\rho_{n_{T,l}, n_{B,l}}\right| = \frac{c}{4\pi f d_{m_l, n_{T,l}}}$; $d_{T,l}$ denotes the center distance between the l-th BS and the l-th ITS.

$$\mathbf{s}_{l,n_{T,l}} = \left[\rho_{n_{T,l},1}\exp\left(-j\frac{2\pi f}{c}(d_{1,n_{T,l}} - d_{T,l})\right), ..., \rho_{n_{T,l},N_{B,l}}\exp\left(-j\frac{2\pi f}{c}(d_{N_{B,l},n_{T,l}} - d_{T,l})\right)\right], \forall l \in [1, L]. \quad (1)$$

C. Overall Algorithm

Based on above discussion in Section III-A and Section III-B, this subsection summarizes the overall algorithm in *Algorithm* 1. Since the LDT and QT are employed to reformulate the sum rate maximization problem by two types of auxiliary vectors, *Algorithm* 1 provides the similar procedures to [11], [22], solving problem (2). Hence, the convergence analysis in [11], [22] can be applied to our work, and is omitted here to conserve space.

Algorithm 1: Overall algorithm to solve (2)

1) **Initialization**: iteration index q, initial points $\mathbf{w}^{(0)}$, $\boldsymbol{\theta}_R^{(0)}$, $\boldsymbol{\theta}_T^{(0)}$, initial objective function $f_1^{(0)}\left(\mathbf{w}^{(0)}, \boldsymbol{\theta}_R^{(0)}, \boldsymbol{\theta}_T^{(0)}\right)$, and algorithm accuracy ι.
2) Repeat: at the q-th iteration
   a) **Update** $\boldsymbol{\nu}$ using (3)
   b) **Update** $\boldsymbol{\omega}$ using (6).
   c) **Update** $\mathbf{w}^{(q+1)}$ using (7).
   d) **Solve** (8) to **update** λ by bisection method.
   e) **Update** $\boldsymbol{\theta}_R^{(q+1)}$ by the ADMM algorithm.
   f) **Update** $\boldsymbol{\theta}_T^{(q+1)}$ by the ADMM algorithm.
   g) **Update** $f_1^{(q+1)}$ and **set** $q = q + 1$ until convergence $\left|f_1^{(q+1)}\left(\mathbf{w}^{(q+1)}, \boldsymbol{\theta}_R^{(q+1)}, \boldsymbol{\theta}_T^{(q+1)}\right) - f_1^{(q)}\left(\mathbf{w}^{(q)}, \boldsymbol{\theta}_R^{(q)}, \boldsymbol{\theta}_T^{(q)}\right)\right| \leq \iota$.
3) **Output**: $f_1^*\left(\mathbf{w}^*, \boldsymbol{\theta}_R^*, \boldsymbol{\theta}_T^*\right)$.

Then, we characterize the computational complexity of *Algorithm* 1 here. We set the iteration number for the convergence of the AO algorithm and the ADMM algorithm with respect to IRS/ITS phase shifts as I_{AO} and $I_{ADMM,R/T}$, respectively. The computational complexity order for optimizing the active beamforming is $K\mathcal{O}\left(N_B^3\right)$; the complexity order of the ADMM algorithm to optimize the IRS/ITS phase shifts is $\mathcal{O}\left(I_{ADMM,R/T}N_T^2 + N_T^3\right)$. Thus, the overall computational complexity of *Algorithm* 1 is $I_{AO}\left[K\mathcal{O}\left(N_B^3\right) + \sum_{p=R}^{T}\mathcal{O}\left(I_{ADMM,p}N_T^2 + N_T^3\right)\right]$.

IV. Simulation Results

This section demonstrates the simulation results to highlight the performance of proposed algorithm in comparison to several benchmarks. Here, we adopt a three-dimensional (3-D) coordinate for the deployment of BS, ITS, IRS, and IoT devices. Specifically, all ITS-assisted BSs are located at $(0, 0, Z_{ITS})$, where Z_{ITS} follows the distribution in [23]; the IRS is located at $(100, 100, 0)$; the coordinate of all IoT devices are randomly distributed in a circle with a radius 50 meters centered at $(200, 0, 0)$. The channel coefficients between ITS-assisted BS and IoT devices, ITS-assisted BS and IRS, as well as IRS and IoT devices, are modelled as Rician fading [23]. The path-loss model is modelled as $\mathcal{PL}_x = A\left(\frac{d_x}{d_{ref}}\right)^{\epsilon_x}$, where $A = -30$ dBm associated with the reference distance $d_{ref} = 1$ metre; d_x and ϵ_x, $x = \{ITS2D, ITS2IRS, IRS2D\}$ between ITS-assisted BS and IoT device, ITS-assisted and IRS, as well as IRS and IoT device, respectively. The bandwidth is set to be 1 MHz [24]. Unless other specified, the remaining network configurations are demonstrated as: $N_{B,l} = 5$, $N_{T,l} = 64$, $L = 5$, $K = 5$, $\sigma^2 = \sigma_k^2 = -90$ dBm, and $P = 30$ dBm. To highlight the performance of the proposed scheme, we consider the following benchmark schemes, i.e., Majorization-Minimization (MM) algorithm [25], random phase shift (RPS) scheme [26], discrete phase shift (DPS) scheme [27], and the scheme without IRS [28] under the same simulation configurations.

First, we examine the impact of the number of BS L on the sum rate performance in Fig. 2, which shows that all of the schemes yield a monotonically increasing behaviour with respect to L, which confirms that a large number of BS can positively affect the sum rate performance of the cell-free system. Although the proposed ADMM-based scheme produces a very close performance to the MM-based scheme, it unconsciously outperforms the MM-based scheme, which confirms its effectiveness. The proposed scheme significantly outperforms that with RPS, DPS (1 or 2 bits)[6], and without IRS, this highlights the optimal ITS/IRS phase shift design.

Next, we examine the sum rate performance versus the element number of each ITS $N_{T,0} = N_{T,l}$, $\forall l \in [1, L]$ in Fig. 3. It can be observed that all schemes have an increasing trend with $N_{T,0}$, it confirms that having a large number of ITS elements positively affects the sum rate. Also, the proposed scheme yields a very close performance to the MM-based scheme, and significantly outperforms that with RPS, with DPS, as well as without IRS, which highlights the importance of optimal phase shift design.

Then, the sum rate versus the number of IRS reflecting element N_R is examined in Fig. 4. Specifically, a large number of IRS reflecting elements can markedly enhance the sum rate performance for all IRS-related schemes, which significantly outperform that without IRS. This validates the effectiveness of IRS. Also, the proposed scheme outperforms the other benchmarks with RPS, DPS, achieves a very similar performance to the MM-based scheme. This confirms the importance of the optimal phase shift design.

Finally, Fig. 5 shows the sum rate versus transmit power budget P. As expected, as P increases, the sum rate demonstrates an monotonically increasing behaviour for all schemes. In addition, the proposed scheme has a very close performance to the MM-based scheme, and has a better performance than the other benchmarks with RPS, with DSP, as well as without IRS. The gap between the proposed scheme and these benchmarks becomes larger when P increases, which confirms that larger transmit power can effectively improve the sum rate performance.

[6]It is clearly seen that the proposed scheme with continuous phase shifts outperforms its quantized counterpart. This is due to the fact that in the scheme with quantized phase shifts, the two-path signals from direct and cascaded links are not able to perfectly align in phase at the users, thus resulting in a performance loss in comparison to that with continuous phase shifts. In addition, a larger number of bits (b) will yield a higher granularity of phase shifts to be selected for signal reflection, which is closer to the continuous counterpart in terms of the sum rate performance.

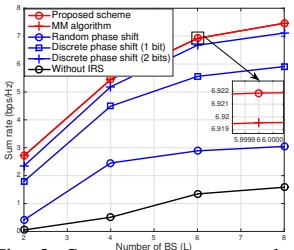

Fig. 2: Sum rate versus number of BS

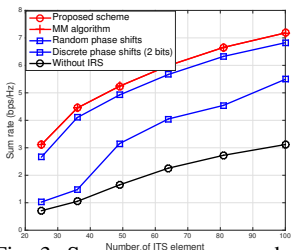

Fig. 3: Sum rate versus number of ITS element.

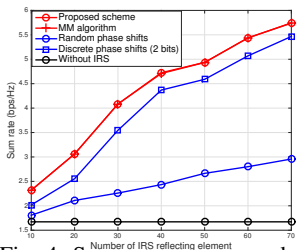

Fig. 4: Sum rate versus number of IRS element.

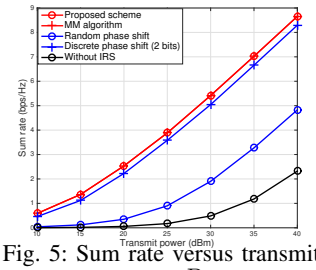

Fig. 5: Sum rate versus transmit power P.

V. Conclusion

This paper investigated the system performance of a joint ITS- and IRS-assisted cell-free network, where the sum rate was maximized by a joint design of the active transmit beamforming at BS, as well as the ITS and IRS passive beampatterns. To solve the non-convex sum rate maximization problem, we considered the LDT and QT to transfer the summation of logarithmically fractional function to the subtractively quadratic form. Then, the AO algorithm was presented to iteratively optimize the active transmit beamforming, as well as the ITS and IRS beampatterns. Specifically, the dual method with bisection search was introduced to derive the active transmit beamfoming, and the ADMM algorithm was adopted to iteratively achieve the closed-form solution of ITS/IRS phase shifts. Finally, numerical results demonstrated the superior performance of the proposed scheme in comparison with benchmarks, such as the MM-based scheme, the DPS scheme, the RPS scheme, and the scheme without IRS. For future works, it is worth investigating: the IRS- and ITS-assisted cell-free MIMO with multi-antenna IoT devices, user association of the ITS-assisted transceiver and IoT devices, as well as the energy efficiency (EE) performance to highlight the advantage of ITS.

References

[1] X. You, C.-X. Wang, J. Huang, X. Gao, Z. Zhang, M. Wang, Y. Huang, C. Zhang, Y. Jiang, J. Wang, *et al.*, "Towards 6G wireless communication networks: vision, enabling technologies, and new paradigm shifts," *Sci. China Inf. Sci.*

[2] Z. Zhu, Z. Chu, and X. Li, *Intelligent Sensing and Communications for Internet of Everything*. Elsevier, Academic Press, 2022.

[3] M. Bashar, K. Cumanan, A. G. Burr, H. Q. Ngo, M. Debbah, and P. Xiao, "Maxmin rate of cell-free massive MIMO uplink with optimal uniform quantization," *IEEE Trans. Commun.*, vol. 67, no. 10, pp. 6796–6815, Oct. 2019.

[4] W. Du, Z. Chu, G. Chen, P. Xiao, Z. Lin, C. Huang, and W. Hao, "Weighted sum-rate and energy efficiency maximization for joint ITS and IRS assisted multiuser MIMO networks," *IEEE Trans. Commun.*, vol. 70, no. 11, pp. 7351–7364, Nov. 2022.

[5] H. Niu, Z. Lin, Z. Chu, Z. Zhu, P. Xiao, H. X. Nguyen, I. Lee, and N. Al-Dhahir, "Joint beamforming design for secure RIS-assisted IoT networks," *IEEE Internet Things J.*, vol. 10, no. 2, pp. 1628–1641, Jan. 2023.

[6] S. Huang, Y. Ye, M. Xiao, H. V. Poor, and M. Skoglund, "Decentralized beamforming design for intelligent reflecting surface-enhanced cell-free networks," *IEEE Wireless Commun. Lett.*, vol. 10, no. 3, pp. 673–677, Mar. 2021.

[7] Y. Zhang, B. Di, H. Zhang, J. Lin, Y. Li, and L. Song, "Reconfigurable intelligent surface aided cell-free MIMO communications," *IEEE Wireless Commun. Lett.*, vol. 10, no. 4, pp. 775–779, Apr. 2021.

[8] X. Ma, D. Zhang, M. Xiao, C. Huang, and Z. Chen, "Cooperative beamforming for RIS-aided cell-free massive MIMO networks," *IEEE Trans. Wireless Commun.*, pp. 1–1, 2023.

[9] Y. Zhang, H. Zhao, W. Xia, W. Xu, C. Tang, and H. Zhu, "How much does reconfigurable intelligent surface improve cell-free massive MIMO uplink with hardware impairments?," *IEEE Trans. Commun.*, pp. 1–1, 2023.

[10] Q. Wu and R. Zhang, "Towards smart and reconfigurable environment: Intelligent reflecting surface aided wireless network," *IEEE Commun. Mag.*, vol. 58, no. 1, pp. 106–112, Jan. 2020.

[11] H. Guo, Y.-C. Liang, J. Chen, and E. G. Larsson, "Weighted sum-rate maximization for reconfigurable intelligent surface aided wireless networks," *IEEE Trans. Wireless Commun.*, vol. 19, no. 5, pp. 3064 – 3076, May 2020.

[12] Z.-Q. He and X. Yuan, "Cascaded channel estimation for large intelligent metasurface assisted massive MIMO," *IEEE Wireless Commun. Lett.*, vol. 9, no. 2, pp. 210–214, Feb. 2020.

[13] Z. Wang, L. Liu, and S. Cui, "Channel estimation for intelligent reflecting surface assisted multiuser communications: Framework, algorithms, and analysis," *IEEE Trans. Wireless Commun.*, vol. 19, no. 10, pp. 6607–6620, Oct. 2020.

[14] L. Wei, C. Huang, G. C. Alexandropoulos, C. Yuen, Z. Zhang, and M. Debbah, "Channel estimation for RIS-empowered multi-user MISO wireless communications," *IEEE Trans. Commun.*, vol. 69, no. 6, pp. 4144–4157, Jun. 2021.

[15] Z. Li, W. Chen, C. He, X. Bai, and J. Lu, "Multi-antenna systems by transmissive reconfigurable meta-surface," *https://arxiv.org/abs/2109.05462*.

[16] G. Zhou, C. Pan, H. Ren, K. Wang, and A. Nallanathan, "A framework of robust transmission design for IRS-aided MISO communications with imperfect cascaded channels," *IEEE Trans. Signal Process.*, vol. 68, pp. 5092–5106, Aug. 2020.

[17] Y. Omid, S. M. Shahabi, C. Pan, Y. Deng, and A. Nallanathan, "Low-complexity robust beamforming design for IRS-aided MISO systems with imperfect channels," *IEEE Communications Letters*, vol. 25, no. 5, pp. 1697–1701, May 2021.

[18] S. Hong *et al.*, "Robust transmission design for intelligent reflecting surface-aided secure communication systems with imperfect cascaded CSI," vol. 20, no. 4, pp. 2487–2501, Apr. 2021.

[19] Z. Zhang, Y. Liu, Z. Wang, X. Mu, and J. Chen, "Physical layer security in near-field communications," *https://arxiv.org/abs/2302.04189*, 2023.

[20] Z. Li, W. Chen, Z. Liu, H. Tang, and J. Lu, "Joint communication and computation design in transmissive RMS transceiver enabled multi-tier computing networks," *IEEE J. Sel. Areas Commun.*, vol. 41, no. 2, pp. 334–348, Feb. 2023.

[21] Z. Chu, P. Xiao, D. Mi, W. Hao, Q. Chen, and Y. Xiao, "IRS-assisted wireless powered IoT network with multiple resource blocks," *IEEE Trans. Commun.*, vol. 71, no. 4, pp. 2335–2350, Apr. 2023.

[22] K. Shen and W. Yu, "Fractional programming for communication systemspart II: Uplink scheduling via matching," *IEEE Transactions on Signal Processing*, vol. 66, no. 10, pp. 2631–2644, May 2018.

[23] Z. Chu, P. Xiao, D. Mi, W. Hao, M. Khalily, and L.-L. Yang, "A novel transmission policy for intelligent reflecting surface assisted wireless powered sensor networks," *IEEE J. Sel. Topics Signal Process.*, vol. 15, no. 5, pp. 1143–1158, Aug. 2021.

[24] N. Li, W. Hao, F. Zhou, Z. Chu, S. Yang, O. Muta, and H. Gacanin, "Min-max latency optimization for IRS-aided cell-free mobile edge computing systems," *IEEE Internet Things J.*, pp. 1–1, 2023.

[25] Z. Chu, Z. Zhu, F. Zhou, M. Zhang, and N. Al-Dhahir, "Intelligent reflecting surface assisted wireless powered sensor networks for internet of things," *IEEE Trans. Commun.*, vol. 69, no. 7, pp. 4877–4889, Jul. 2021.

[26] C. Pan, H. Ren, K. Wang, M. Elkashlan, A. Nallanathan, J. Wang, and L. Hanzo, "Intelligent reflecting surface aided MIMO broadcasting for simultaneous wireless information and power transfer," *IEEE J. Sel. Areas Commun.*, vol. 38, no. 8, pp. 1719–1734, 2020.

[27] Q. Wu and R. Zhang, "Beamforming optimization for wireless network aided by intelligent reflecting surface with discrete phase shifts," *IEEE Trans. Commun.*, vol. 68, no. 3, pp. 1838–1851, 2020.

[28] Q. Wu and R. Zhang, "Intelligent reflecting surface enhanced wireless network via joint active and passive beamforming," *IEEE Trans. Wireless Commun.*, vol. 18, no. 11, pp. 5394–5409, Nov. 2019.